Water Science & Technology

Water Science & Technology Vol 85 No 4, 1218 doi: 10.2166/wst.2022.021

Surface modification of spent coffee grounds using phosphoric acid for enhancement of methylene blue adsorption from aqueous solution

M. S. Akindolie[a] and H. J. Choi[b,*]

[a] Research Center for Marine Bio-Food and Medicine, Catholic Kwandong University, Beomil-ro 579 Beon-gil, 25601 Gangneung-si, Republic of Korea
[b] Department of Biomedical Science, Catholic Kwandong University, Beomil-ro 579 beon-gil, 25601 Gangneung-si, Republic of Korea
*Corresponding author. E-mail: hjchoi@cku.ac.kr

HJC, 0000-0003-3370-4277

ABSTRACT

In this study, the surface of the spent coffee grounds (SCG) was activated using phosphoric acid to increase the removal efficiency of methylene blue (MB) in aqueous solution, which is one of the harmful substances emitted in industrial processes. According to Fourier transform infra-red analysis, after phosphorylation of the SCG (PSCG), $P=O$ group, P–O–C (aromatic) bond, $P=OOH$ and P–O–P were newly introduced on the surface of the adsorbent, and the peaks of carboxyl groups and OH-group were large and broad. In addition, the surface area and mesopore range of the PSCG adsorbent were increased, and the structure changed, which enabled easy adsorption of MB. The process of adsorbing MB from aqueous solution using PSCG was more suitable for the pseudo-second order and Langmuir models, and the adsorption process was closer to chemisorption than physical adsorption. The maximum adsorption capacity of PSCG was 188.68 mg/g. As a result of the reuse test, PSCG showed excellent performance with a high removal efficiency of 90% up to four consecutive uses. PSCG modified with phosphoric acid, an abundant lignocellulose-based biosorbent that is readily available everywhere, is a promising adsorbent capable of adsorbing MB in aqueous solution.

Key words: adsorption, lignocellulose, methylene blue, phosphorylation, spent coffee grounds

HIGHLIGHTS

- Spent coffee grounds activated using phosphoric acid (PSCG) for removal of methylene blue.
- After phosphorylation surface area and mesopore range were increased.
- Maximum adsorption capacity of PSCG was 188.68 mg/g.
- PSCG showed a high removal efficiency of 90% up to four consecutive uses.
- Surface complexing mechanism between the oxygen-containing functional group and MB ions.

GRAPHICAL ABSTRACT

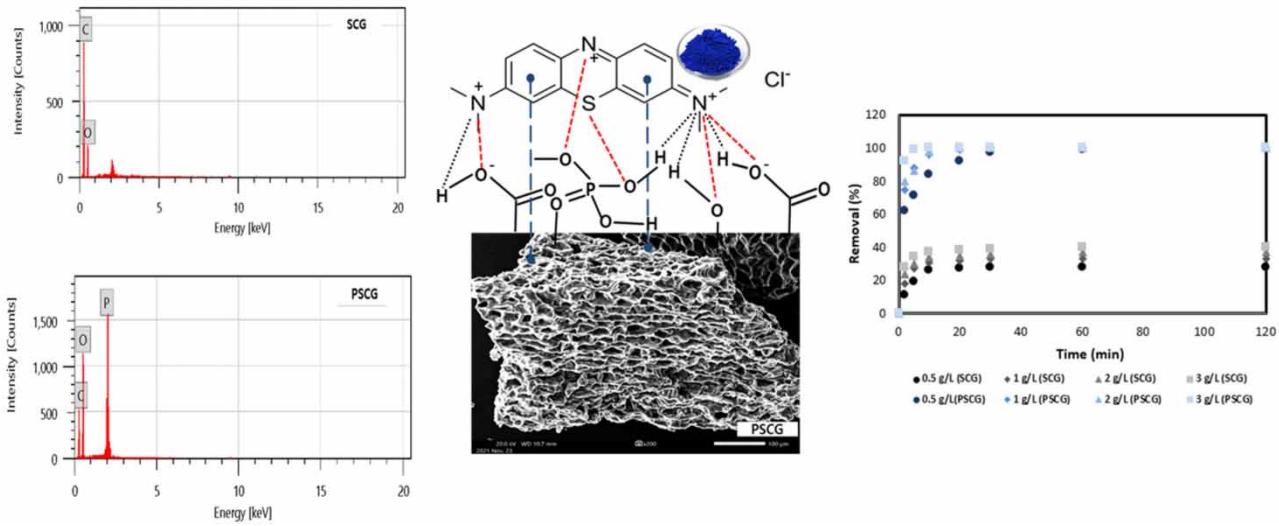

INTRODUCTION

With the development of various industries, the dye market has also grown tremendously, which is directly related to water pollution. Dyes account for the largest proportion of water pollutants. Among the various dyes, one notable organic dye is methylene blue (MB), which is widely applied in textiles, chemical indicators, dyeing, printing, pesticides, paper coatings, cosmetics, and pharmaceuticals (Choi & Yu 2019). MB is a heterocyclic aromatic compound and exists in the form of three water molecules bonded to one MB molecule in aqueous solution (Han *et al.* 2020). In addition, MB contains an aromatic ring; it is toxic and carcinogenic (Lee & Choi 2021). Therefore the removal of MB from an aqueous environment is necessary to maintain water quality and a green environment.

Lignocellulose-based activated carbon is also being studied to adsorb harmful substances by reforming activated carbon with clay (Khnifira *et al.* 2022), metal (Arora *et al.* 2019; Soni *et al.* 2020a; Karami *et al.* 2022), and metal oxide (Patil & Shrivastava 2016; Soni *et al.* 2020b; Kumar & Kumar 2022). However, most are produced through two main processes: carbonization or pyrolysis and activation (physical or chemical). Physical pretreatment includes mechanical destruction, boiling, heating, autoclaving, freeze drying, or vacuuming (Basu *et al.* 2018). However, the adsorbent through physical pretreatment has disadvantages in that the treatment efficiency of harmful substances in aqueous solution is low and selective adsorption is difficult (Han *et al.* 2020). Therefore, recently, many researchers have activated the surface of the adsorbent by attaching a functional group that is beneficial to the adsorption of harmful substances using chemicals such as acids and bases. As a result, it has been possible to selectively adsorb harmful substances, and the adsorption efficiencies have been reported to increase (Kouzbour *et al.* 2019; Lee & Choi 2021; Misran *et al.* 2022). Choi *et al.* (2021) reported that the carboxyl group (–COOH) of the orange peel adsorbent modified with sulfonic acid was increased, thereby improving the Cu(II) adsorption efficiency. Also, Chen *et al.* (2021) reported that introducing a carboxylic acid functional group (–COOH) on the surface of the spent coffee grounds (SCG) provides a higher binding capacity to adsorb heavy metal ions. This is because acidic functional groups on the surface of the adsorbent such as phenol, carboxyl, hydroxyl and carbonyl functional groups of the SCG adsorbent modified with sulfonic acid were removed by binding with heavy metal ions (Leng *et al.* 2019; Elgarahy *et al.* 2021).

One of the promising lignocellulose-based activated carbon precursors is coffee grounds. Coffee is loved by many people around the world, the second most consumed beverage in the world after water; it is sold with an average of billions of cups per day, and it is known that 6 million tons of soluble coffee are produced annually (Choi *et al.* 2021). Due to this, a large amount of SCG is produced, and it is expected that the amount of SCG produced every year will steadily increase with the growth of the coffee industry. SCG is a lignocellulosic material composed of lignin (27.5%), cellulose (45.6%), and hemicellulose (21.3%) (Choi *et al.* 2021; Shi *et al.* 2021). Adsorption of hazardous substances using SCG has a very useful value in terms of recycling waste. So far, many studies (Choi *et al.* 2021; Elgarahy *et al.* 2021; Qiao *et al.* 2021) have been published on the adsorption of various heavy metals using SCG, but there have been very few papers on the phosphorylation of SCG to

remove MB from aqueous solution and analyze the removal efficiency. Phosphoric acid in aqueous solution, on the one hand, promotes the bond cleavage reaction and, on the other hand, promotes crosslinking through cyclization and condensation to form a bond layer such as phosphate and polyphosphate ester, which can protect the internal pore structure (Leng *et al.* 2019; Guediri *et al.* 2020; Elgarahy *et al.* 2021). These reactions can act as excellent MB adsorbents in aqueous solutions. According to previous studies (Xu *et al.* 2014; Basu *et al.* 2018; Han *et al.* 2020; Zeng *et al.* 2021), phosphoric acid-activated adsorbents can be recycled and have various advantages such as low toxicity. Therefore, in this study, to increase the removal efficiency of MB in aqueous solution, SCG was modified and activated using phosphoric acid. For the optimization of MB removal efficiency, various parameters (initial pH, contact time, initial concentration of MB, capacity of adsorbent) were evaluated. The experimental data were analyzed by adsorption isotherms, and the properties and adsorption kinetics of the adsorbent were used to explain the adsorption mechanism.

MATERIALS AND METHODS

Materials

Phosphorylation of spent coffee ground

SCG was collected at a coffee shop in Gangneung, and ground with a particle size of less than 40–60 mesh (0.25–0.4 mm) were recovered and washed several times with distilled water to remove contaminants. The washed SCG was dried at 75 $\pm$ 2 °C for 24 hours to evaporate moisture. The pretreated SCG was stored in a desiccator for activation with phosphoric acid.

The method for activating SCG into porous carbon using phosphoric acid (H_3PO_4) is as follows. First, 200 mL of phosphoric acid (85%) and 75 g of phosphorus pentoxide were mixed and completely dissolved while heating and stirring and then cooled at room temperature. A 100 g sample of dried SCG (40–60 mesh) was added to the prepared phosphoric acid solution (300 mL), and a phosphorylation reaction was induced while stirring at 150 rpm for 5 hours using a cylindrical reactor (3 L). The mixed sample was left at room temperature for 4 hours to allow the reaction to occur completely, then the pH was adjusted to neutral by adding 1 N sodium hydroxide, washed thoroughly with distilled water, and dried for 24 hours in a dryer. Phosphorylated SCG (PSCG) was stored in a desiccator for use in experiments.

Adsorbate

Methylene blue (MB; $C_{16}H_{18}ClN_3S{\cdot}3H_2O$, molar mass: 319.85 g/mol, Sigma-Aldrich, USA) is a basic dye. The hydrate is blue and exists in the form of three water molecules bonded to each MB molecule. MB was used in powder form. After preparing the 1,000 mg/L concentration, it was then diluted with distilled water to prepare a solution of the required concentration.

Experiment and analytical method

Characterization of SCG and PSCG

The surface images were taken of PSCG and SCG using scanning electron microscopy (SEM, JSM-IT500, JEOL Ltd Japan) and the chemical composition of the adsorbent were analyzed using energy-dispersive X-ray spectroscopy (EDS, JSM-IT500, JEOL Ltd Japan). Fourier transform infrared (FT-IR) spectroscopy (Perkin Elmer, FT-IR 1760X, USA) was applied in a scan range of 400–4,000 cm^{-1} to investigate the presence of functional groups of SCG and PSCG. Brunauer–Emmett–Teller (BET) surface area was examined using a BET Surface Analyzer (Quantachrome Instruments version 11.03) via adsorption/desorption isotherms of N_2 performed at 77 K. After the adsorption process, the morphology, functional groups and BET surface area of the dried PSCG were also examined to compare before and after adsorption. pHpzc was analyzed according to the method reported in a previously published study (Choi *et al.* 2021). The amount of adsorbent was measured using an electronic balance (XP26, Mettler Toledo, Swiss), and the pH was measured using a pH meter (SevenGO pro, Mettler Toledo).

Parametric study

During the adsorption experiment, all solutions were diluted with distilled water according to a predetermined concentration. All experiments were performed as batch tests. In previous studies of MB removal using PSCG, the optimal pH was 7, which is neutral, and the temperature was room temperature (Choi & Yu 2019; Choi *et al.* 2021). Therefore, experiments according to temperature and pH were excluded. To investigate the effect of the amount of PSCG on the adsorption efficiency of MB, the experiment was conducted with adsorbent amounts between 0.5–3 g/L), the concentration of MB of 20 mg/L, pH 7, and

room temperature. In the adsorption efficiency experiment with respect to the initial concentration of MB, the concentration of MB was adjusted to 5–200 mg/L. The contact time of all experiments was 0–120 min, pH 7, and sampling was performed at a set time (0, 2, 5, 10, 20, 30, 60, 120 min) while stirring at 120 rpm in a shaking incubator. The amount of MB was measured in the samples collected at a set time using a UV–VIS spectrophotometer (Shimadzu 1800, Japan), and the adsorption amount and adsorption efficiency were calculated using Equations (1) and (2) below:

$$q_t = \frac{(C_0 - C_t)V}{m} \tag{1}$$

$$R = \frac{(C_0 - C_e)}{C_0} \times 100 \tag{2}$$

where R is MB removal efficiency in aqueous solution.

To select appropriate kinetic and isotherm models for MB adsorption process, Chi-squared (χ^2) was calculated using Equation (3):

$$\chi^2 = \sum_{i=1}^{n} \frac{(q_{e,exp} - q_{e,cal})^2}{q_{e,cal}} \tag{3}$$

where $q_{e,exp}$ and $q_{e,cal}$ are equilibrium adsorption capacity obtained from experiments and models, respectively.

Adsorption kinetics and isotherm

Adsorption capacity experiments according to various initial concentrations were analyzed using adsorption kinetics (pseudo-first-order (PFO) and pseudo-second-order (PSO)) and adsorption isotherms (Langmuir, Freundlich and Temkin). Table 1 summarizes the mathematical equations and linearized forms of adsorption kinetics and adsorption isothermal equations.

Table 1 | Adsorption kinetic, isotherm and thermodynamic models

Model	Equation	Parameters
PFO	$\ln(q_e - q_t) = \ln q_e - k_1 t$	q_t: amount of adsorbate adsorbed at time (mg/L) q_e: equilibrium adsorption capacity (mg/g) k_1: pseudo-first-order rate constant (1/min) t: time (min)
PSO	$\frac{t}{q_t} = \frac{1}{k_2 \cdot q_e^2} + \frac{t}{q_e}$	k_2: pseudo-second-order rate constant (L/mg·min)
Intra particle diffusion	$q_t = k_{id} t^{1/2} + C$	k_{id}: Intraparticle diffusion rate constant (mg/(g·min$^{1/2}$)) C: intercept (mg/g)
Langmuir	$\frac{1}{q_e} = \frac{1}{q_m K_L}\frac{1}{C_e} + \frac{1}{q_m}$ $R_L = \frac{1}{1 + K_L C_0}$	q_m: maximum adsorption capacity (mg/g) K_L: Langmuir constant (L/mg) C_e: equilibrium adsorbate concentration in solution (mg/L) C_0: initial adsorbate concentration in solution (mg/L) R_L: separation factor
Freundlich	$\ln q_e = \ln K_F + \left(\frac{1}{n}\right)\ln C_e$	K_F: Freundlich constant (mg/g(L/mg)$^{1/n}$) n: heterogeneity factor
Temkin	$q_e = B \ln K_T + B \ln C_e$	K_T: Temkin equilibrium binding constant (L/mg) B: Temkin constant (J/mol)
Gibbs free energy	$\Delta G° = \Delta H° - T\Delta S°$	$\Delta G°$: Gibbs free energy change (kJ/mol) $\Delta H°$: Change of enthalpy (kJ/mol) $\Delta S°$: Change of entropy (kJ/mol·K) T: Temperature (K)

Reusability

To test the reusability of PSCG, resorption experiments were performed six times using the same PSCG. As initial solutions, 50 mg/L MB solution and 1 g/L PSCG were prepared. The initial solution was reacted with PSCG for 120 minutes, sampled, measured with a UV spectrophotometer (Shimadzu 1800, Japan), and the removal efficiency was calculated using Equations (1) and (2). After the first reaction experiment, PSCG was dried in an oven at 75 °C for 3 hours, and the same conditions as the initial experiment were used. The PSCG adsorbent reuse experiment was repeated with the same procedure as the first up to six times without a desorption step.

RESULTS AND DISCUSSION

Characteristics of adsorbent

Surface morphology

The surface morphology of SCG and PSCG was obtained using SEM (Figure 1(a)). Compared with SCG, PSCG was detected to have increased pores, with the rough surface while the size and shape were heterogeneously changed. This surface morphology provides a great advantage for adsorption, because it can provide more adsorption sites for binding the adsorbate. According to the EDS analysis, it was revealed that the carbon content decreased, but the oxygen and phosphorus contents clearly increased (Figure 1(b)). As the adsorption of MB ions by the modified PSCG was achieved by a surface complexation mechanism between MB ions and oxygen-containing functional groups including phosphorus, an increase in oxygen content and an increase in phosphorus have a favorable effect on MB adsorption.

FT-IR spectra

The FT-IR spectra of SCG and PSCG showed broadening and strengthening of certain bands according to the activation, but there was no significant difference in the basic spectra (Figure 1(c)). SCG contains OH aromatics (950–1,300 cm^{-1}), CH-stretching (1,400–1,450 cm^{-1}), C = O carboxylic acids (1,630–1,750 cm^{-1}), CH-stretching of alkane groups (2,800–2,950 cm^{-1}) and carboxyl, phenol or hydrogen-bonded hydroxyl groups in alcohols (3,100–3,600 cm^{-1}).

Conversely, PSCG contains N-containing bioligands (400–500 cm^{-1}), C = C aromatic compounds (625–730 cm^{-1}), OH aromatics and N-H groups (805–910 cm^{-1}), P = O groups, and carboxyl groups (1,007–1,110 cm^{-1}) and $(RO)_3P$ = O (1,300–1,500 cm^{-1}) were either newly created or broadened. In particular, the 1,017–1,100 cm^{-1} and 1,300–1,500 cm^{-1} peaks were deeper and broader than that of SCG because phosphate groups were attached there. These peaks are characteristic of phosphorus and phosphorus–carbon compounds such as phosphates or hydrogen bonds of polyphosphates (P = O groups, P-O-C (aromatic) bonds and P = OOH etc.) present in phosphoric acid-activated carbon (Leng *et al.* 2019; Choi *et al.* 2021; Yang *et al.* 2020). In addition, the peak at 1,000–1,110 cm^{-1} may be due to the symmetrical vibrations of the P + O– of the acidic phosphate ester and the P–O–P of the polyphosphate chain (Chen *et al.* 2021; Elgarahy *et al.* 2021; Qiao *et al.* 2021). Summarizing the above results, as a result of reforming SCG with phosphoric acid, the number of functional groups increased, and the functional groups required for MB adsorption became wider or deeper. This is because the aliphatic residue contained in SCG was destroyed due to phosphorylation of SCG. However, the 3,100–3,700 peak was decreased in PSCG because the carbon content decreased after phosphoric acid activation of SCG (see Figure 1(b)).

Moreover, the FT-IR spectra for PSCG after MB adsorption showed some functional groups derived from MB. Some of the new peaks are the chromophores NH (996 cm^{-1}), C-S (758 cm^{-1}), and the broad bands of C = C, C = O, C = S, C = N from MB were indicated between 1,240–1,780 cm^{-1}. The presence of these functional groups can be used as evidence that MB is adsorbed to PSCG. The decrease in peak height and shift in peak position also confirm that the adsorbent and adsorbate have a strong interaction. Phosphorylation of SCG increases the surface area and porosity of the adsorbent as well as the presence of functional groups such as aromatic rings, –C = O, –C–O–C–, –OH, –C = N, –P = O, –P–O–C, and P = OOH play important roles in increasing MB adsorption capacity in aqueous solution. The surface of PSCG modified with phosphoric acid contains a significant amount of phosphorus-compounds. IR spectra of SCG-derived carbons show multiple functions observable for other carbons obtained by phosphoric acid activation of lignocellulose precursors.

Physical property

Table 2 summarizes the component analysis results of SCG and PSCG. As the O/C ratio increases, the anionic properties of the bio-adsorbent were strengthened due to the increase in the carboxylate groups on the surface of the adsorbent, which tends to increase the adsorption capacity of cationic substances (Choi & Yu 2019; Choi *et al.* 2021). After phosphorylation

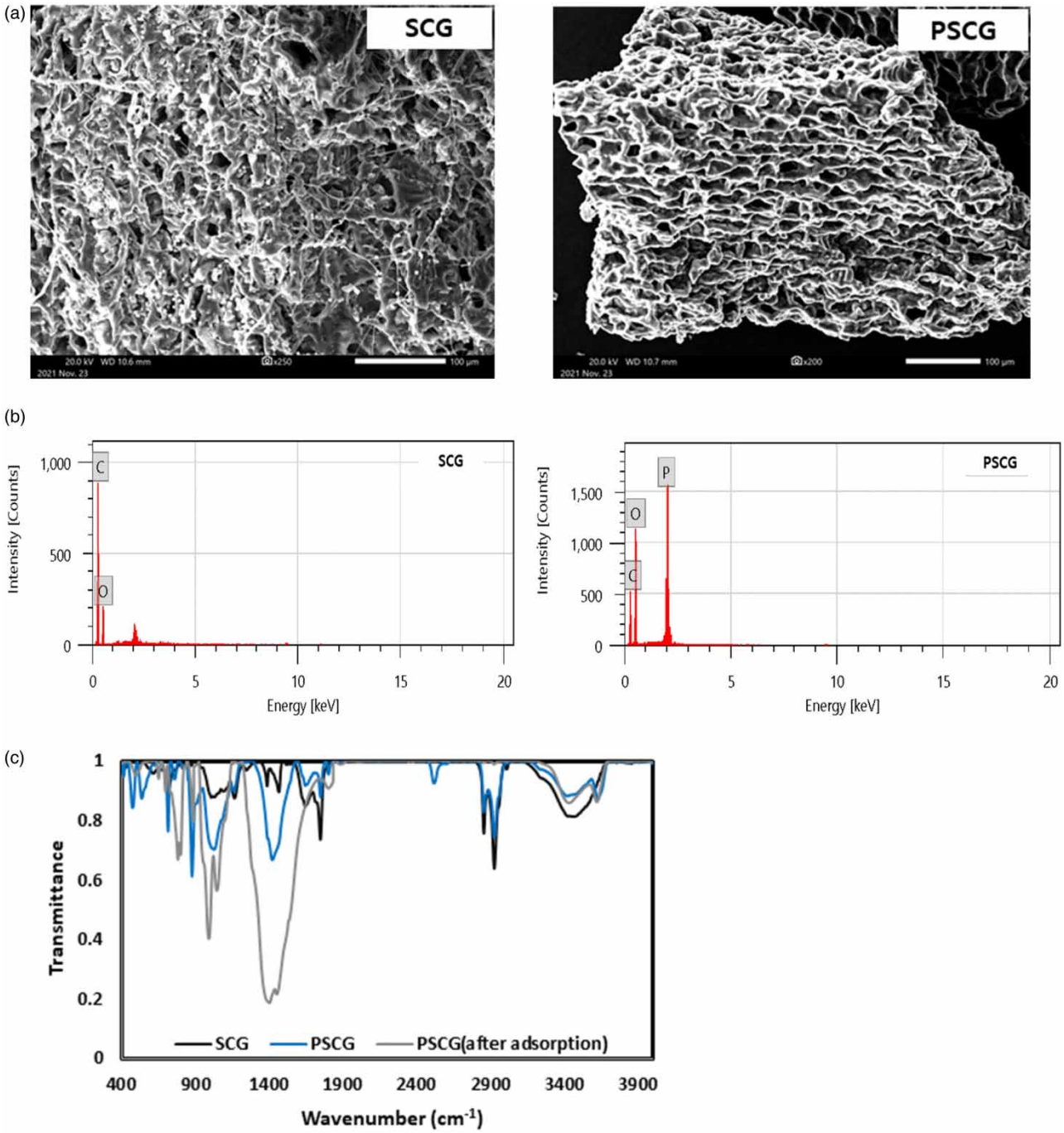

Figure 1 | (a) SEM image for SCG and PSCG. (b) EDS for SCG and PSCG. (c) FT-IR spectra.

of SCG, the O/C ratio increased from 0.49 to 0.97. This proves that the carboxyl group inside the adsorbent increased after the phosphorylation of SCG.

In SCG, 86.7% of micropores and 12.9% of mesopores had more ultrafine pores than mesopores. However, after activation with phosphoric acid, the range of mesopores increased to 96.9%, confirming that the overall pore size of the adsorbent increased. In the activation step of SCG using phosphoric acid, the high molecular compounds contained in SCG were destroyed into small molecules, and the pore size increased. As previously reported (Qiao *et al.* 2021) for the activation process of other lignocellulosic precursors, it is hypothesized that H_3PO_4 reacting within the inner cellulosic structure induces

Table 2 | Physico-chemical characteristic of spent coffee ground (SCG) and phosphorylated spent coffee ground (PSCG) (unit: %)

Component (mass %)	SCG	PSCG	PSCG (after adsorption)
C	66.97	47.12	–
O	33.03	45.48	–
Pore size (nm)			
< 2	86.7 ± 2.9	2.6 ± 0.7	2.1 ± 0.1
2–50	12.9 ± 0.5	96.9 ± 2.1	95.2 ± 1.7
> 50	0.4 ± 0.01	0.5 ± 0.02	3.7 ± 0.8
BET surface area (m^2/g)	8.27	662.38	658.12
Pore volume (cc/g)	0.021	0.377	0.368

depolymerization leading to enhancement of the pore volume, leading to overall volume expansion. The size of PSCG pores after MB adsorption showed little change in the size of 2–50 nm. However, it decreased below 2 nm and increased above 50 nm, resulting in an overall increase in the pore size of PSCG. The pore size of PSCG increased above 50 nm, resulting in an overall increase in PSCG pores. This is because the pores of PSCG were filled with MB dye molecules after MB adsorption and the pore size increased.

The results of BET measurement (Table 2) show the characteristics of SCG and PSCG. The surface area was significantly increased in PSCG compared to SCG. The activation process of SCG using phosphoric acid successfully enlarged the pores of SCG. This is considered to increase the surface area of PSCG as long-chain polymers such as aliphatic are destroyed by phosphoric acid, as observed in FT-IR analysis. The high surface area of PSCG provides sufficient active sites for MB dye adsorption. However, the surface area of PSCG decreased after adsorption because MB dye molecules were adsorbed on the PSCG surface and covered the pores. Due to this, the pore volume of PSCG was also reduced after MB adsorption.

Point of zero charge (pzc)

The pH, together with the size and temperature of the adsorbent pore size and the amount of adsorbent, is a major factor affecting bio-adsorption (Choi *et al.* 2021). This is because the optimal pH value for a specific biosorbent process depends on the zero point charge value (pHpzc) of the biosorbent and the target metal ion (Basu *et al.* 2018; Kouzbour *et al.* 2019). pHpzc is the pH (of the solution) value at which the surface charge of the biosorbent becomes zero (Choi & Yu 2019; Lee & Choi 2021). Proton binding by all carbons exhibits positive (proton adsorption) and negative (proton emission) moieties (Sych *et al.* 2012; Choi *et al.* 2021). At a pH above pHpzc, the surface of the adsorbent becomes negatively charged, and the electrostatic interaction with the positively charged adsorbent material is strong, increasing the adsorption efficiency (Xu *et al.* 2014; Han *et al.* 2020). When phosphoric acid is added to SCG, carbon with an acidic surface is formed, which shows that the pHpzc significantly decreases from 6.43 to 3.96 in the acidic region (Figure 2(a)). It can be seen that the acidic group was strongly attached to the surface of PSCG. In addition, it means that the pH range that can accommodate the adsorption of MB ions in aqueous solution was widened, which may lead to an increase in adsorption capacity.

Parametric study

Effect of adsorbent dose

In order to examine the adsorption efficiency of MB according to the amount of SCG and PSCG, the experiment was performed at the adsorbent rate of 0.5–3 g/L, the concentration of MB at 20 mg/L, pH 7, and 25 °C. The results are shown in Figure 2(b). In both SCG and PSCG, as the amount of adsorbent increased, the time to reach the maximum adsorption amount shortened, and the total adsorption amount of MB in aqueous solution increased. The removal of MB from the aqueous solution proceeded very rapidly during the first 10 minutes, and then the removal rate was slowed until equilibrium was reached. The rapid removal of MB at the beginning of the reaction is probably due to a large number of vacant sites available for adsorption. With 1 g/L of PSCG adsorbent, 99% removal is possible within 20 minutes. Also, when using PSCG, MB was completely removed at 60 min by all adsorbent doses experimented in this study. The adsorption efficiency of MB for PSCG was about 2.5–3.5 times higher than that of SCG, and it can be confirmed that the maximum adsorption was reached within a short time. This result is thought to be because, as already mentioned in the analysis of the physical property and the surface

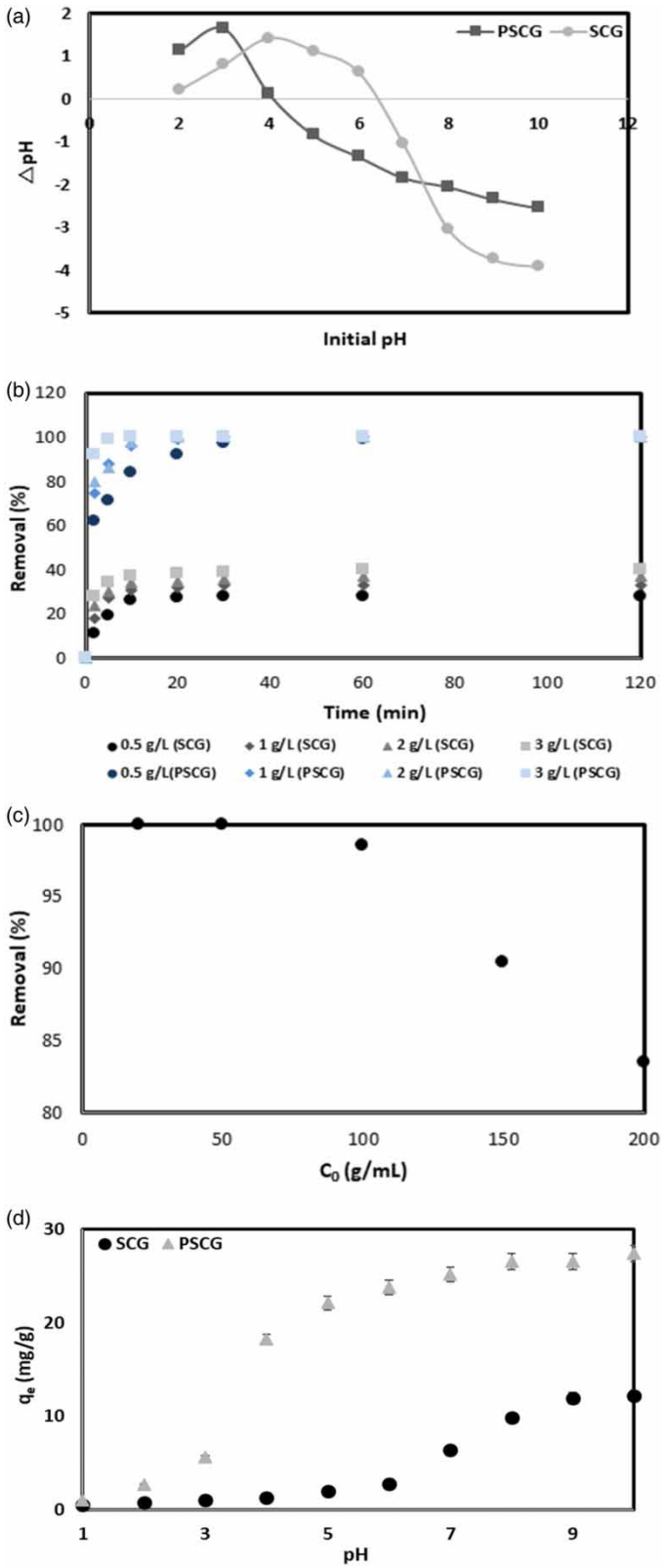

Figure 2 | (a) Change of pHpzc; (b) various adsorbent doses; and (c) various adsorbent doses; (d) different pH for MB adsorption by SCG and PSCG.

morphology of the adsorbent, the introduction of various functional groups and phosphate groups on the surface of the adsorbent. Also, the increase in the surface area of the adsorbent after phosphorylation gave favorable adsorption of MB. These results are consistent with the research results of many researchers who reformed agricultural waste to adsorb heavy metals in aqueous solutions (Yang *et al.* 2020; Liu *et al.* 2021b; Qiao *et al.* 2021; Misran *et al.* 2022).

In general, as the amount of biosorbent increases, the adsorption capacity of heavy metals increases (Zhuang *et al.* 2020). This is because the number of active sites capable of adsorbing the adsorbate increases as the amount of adsorbent increases (Leng *et al.* 2019; Zhang *et al.* 2021). However, according to the results of several previous experiments (Basu *et al.* 2018; Yang *et al.* 2020; Choi *et al.* 2021; Elgarahy *et al.* 2021), it was observed that, after reaching the maximum adsorption efficiency, the adsorption capacity did not increase but even started to decrease even when the amount of biosorbent was increased. The reason is that if too much biosorbent is administered, the biosorbent particles are agglomerated. As a result, the active sites of the adsorbent overlap each other, and mass transfer is blocked. To solve these problems, increasing the stirring speed of the aqueous solution helps to overcome the mass transfer resistance, but it is necessary to optimize the stirring speed because if the stirring speed is too high, fragmentation of the biosorbent may occur.

Effect of initial concentration

According to the experimental results of the amount of adsorbent, it was found that the adsorption efficiency of MB using PSCG was significantly higher than that of SCG. The efficiency at which the various initial concentration of MB was adsorbed onto PSCG was specifically evaluated with 1 g of adsorbent. As the concentration of the MB concentration in the solution increased, the removal efficiency decreased, but the adsorption capacity increased. The adsorption of MB onto PSCG at an initial concentration of less than 150 mg/L showed a high removal efficiency of over 90%. Even at a concentration of 200 mg/L, a removal efficiency of 83.5% and a maximum adsorption capacity of 167.52 mg/g were obtained. These results are shown in Figure 2(c), which is used to obtain a suitable isothermal adsorption model.

Effect of pH

To examine the effect of pH on the adsorption efficiency of MB, the pH was controlled from 1 to 10 by a 1 g/L adsorbent dose at 25 $\pm$ 1 °C. MB removal in aqueous solutions increased rapidly for PSCG from pH 4 and SCG from pH 7 (Figure 2(d)). This phenomenon was related to the value of pHpzc mentioned above. In addition, as the pH increased, the sulfonic acid, carboxyl, and phenolic hydroxyl groups of the PSCG and SCG adsorbents were deprotonated to form –P = O, –P–O–C, P = OOH, R–COO–, and R–O– groups. Due to this, the surfaces of the PSCG and SCG adsorbents became negatively charged, improving the electrostatic attraction between PSCG and SCG adsorbents and MB ions in aqueous solutions.

Adsorption kinetics and adsorption isotherm

Adsorption kinetics

The linear model has a simple interpretation of the parameter and can relatively easily calculate correlation coefficients (R^2) compared with nonlinear model (Choi & Yu 2018). Therefore, in statistical modeling, which emphasizes the interpretation of the model, linear models are mainly used. In this paper, three linear kinetic models (pseudo-first-order (PFO), pseudo-second-order (PSO) and intraparticle diffusion) were applied to predict the kinetic involved during the present adsorption process. Analysis of the adsorption kinetic model can help to understand the physicochemical interaction between the MB and PSCG, the mass transport, and the adsorption rate, which are necessary to determine the optimal conditions for the adsorption process. In PFO, the adsorption site occupancy is directly proportional to the number of vacant adsorption sites (Amel *et al.* 2012; Khnifira *et al.* 2022). However, in PSO, the adsorption of harmful substances is considered a function of the number of free active sites and the number of ionized substances in the solution (Gomora-Hernandez *et al.* 2020). The analysis results of adsorption kinetics are represented in Table 3, and shown Figure 3(a) and 3(b). To obtain an appropriate kinetic model, the adsorption capacity was be analyzed using different concentrations of MB solutions with different contact times.

The adsorption kinetics showed that the values of $q_{e,cal}$ of PSO were closer to those of $q_{e,exp}$. The value of the correlation coefficient (R^2) of PSO was higher, and the value of χ^2 was lower than that of PFO. Therefore, the MB adsorption process in aqueous solution using PSCG was closer to PSO than to PFO. Moreover, the adsorption rate constant k_2 was higher than that of k_1, confirming that the adsorption rate-determining steps were diffusion and sorption of MB ions into the pores of PSCG. Many studies (Choi & Yu 2019; Leng *et al.* 2019; Choi *et al.* 2021; Elgarahy *et al.* 2021; Zhang *et al.* 2021) have reported that

Table 3 | Parameters of kinetics model and isothermal model for the adsorption of MB onto PCSG

		Concentration (mg/L)			
Parameters		**50**	**100**	**200**	**300**
$q_{e,exp}$		48.9	98.5	167.4	185.6
PFO	$q_{e,cal}$	42.02	94.40	174.16	180.89
	k_1	−0.0327	−0.0393	−0.0445	−0.0446
	R^2	0.6687	0.982	0.9867	0.9748
	χ^2	2.2132	1.3123	1.3002	1.4867
PSO	$q_{e,cal}$	50.05	101.17	172.31	183.01
	k_2	7.9041e−6	9.3792e−7	1.7514e−7	1.4929e−7
	R^2	0.9994	0.9905	0.9427	0.982
	χ^2	1.0236	1.1236	1.2862	1.2342
Intra particle diffusion	k_{id}	0.4173	1.1569	2.2395	2.2803
	C	73.513	55.412	40.536	30.386
	R^2	0.4494	0.6291	0.6587	0.567
Isotherm	Parameters				
Langmuir	q_m		K_L	R^2	
	188.68		39.56	0.999	
Freundlich	K_F		n	R^2	
	111.45		3.63	0.9225	
Temkin	B		K_T	R^2	
	29.45		84.13	0.98	

MB adsorption follows the PSO kinetic model. Moreover, the values of k_1 and k_2 of PFO and PSO decreased as the MB concentration increased, and the adsorption rate of MB onto PSCG decreased as the MB concentration increased.

The plot of q_t versus $t^{1/2}$ for MB adsorption onto PSCG (Figure 3(c)) did not pass through the origin, therefore intraparticle diffusion was not the only rate-limiting step. There were three adsorption processes (film diffusion, pore diffusion and intraparticle transport) of adsorbate onto adsorbent (Choi & Yu 2018). The slowest of the three steps controls the overall rate of the process. As found in this study, pore diffusion and intraparticle diffusion are often rate limiting in a batch experiment. The calculated value of k_{id} and C from the slopes of the plots increased when increasing the MB concentration in the aqueous solution. The larger the value of C representing the thickness of the boundary layer, the greater the contribution of surface sorption in the rate-controlling step.

Adsorption isotherm

According to the Langmuir model, adsorption can only occur in a monolayer manner, in which only a single layer of molecules is attached to the surface of the biosorbent (Choi *et al.* 2021; Zhang *et al.* 2021). The Freundlich model has a heterogeneous surface of the biosorbent and the adsorption is expressed as a multilayer with different intermolecular interactions (Choi & Yu 2019). It is particularly suitable for application when the concentration of the adsorbent in the aqueous solution is low (Amel *et al.* 2012; Lee & Choi 2021). The Temkin isotherm is used to evaluate the relationship between the biosorbent surface and the heat of adsorption of all molecules, showing that the heat of adsorption of all molecules decreases linearly with increasing biosorbent surface coverage (Basu *et al.* 2018; Leng *et al.* 2019). The R^2 of the Freundlich model is lower than that of the Langmuir model. Therefore, the interaction between PSCG and MB is performed as a monolayer adsorption that attaches to the biosorbent surface, with the main adsorption as hypothesized by the Langmuir model. Similar findings have been mentioned in several previous studies (Zieliński *et al.* 2019; Zhuang *et al.* 2020; Choi *et al.* 2021; Zhang *et al.* 2021). However, R^2 of both the Freundlich and Langmuir models was found to be higher than 0.9 (Table 3), so the adsorption of MB using PSCG can be explained as monolayer and multilayer adsorption, applying to both models. Freundlich's K_F indicates that the larger the value, the better the adsorption ability, and the $1/n$ value is 0.1–0.5 (excellent adsorption process), $1/n = 0.5$–1 (the process is easily adsorbed), and $1/n \geq 1$ (the process is difficult to adsorb) (Choi *et al.* 2021; Misran *et al.* 2022). The value of K_F and 1/n calculated from Figure 4 was obtained as 111.45 ((mg/g) $(L/mg)^{1/n}$)

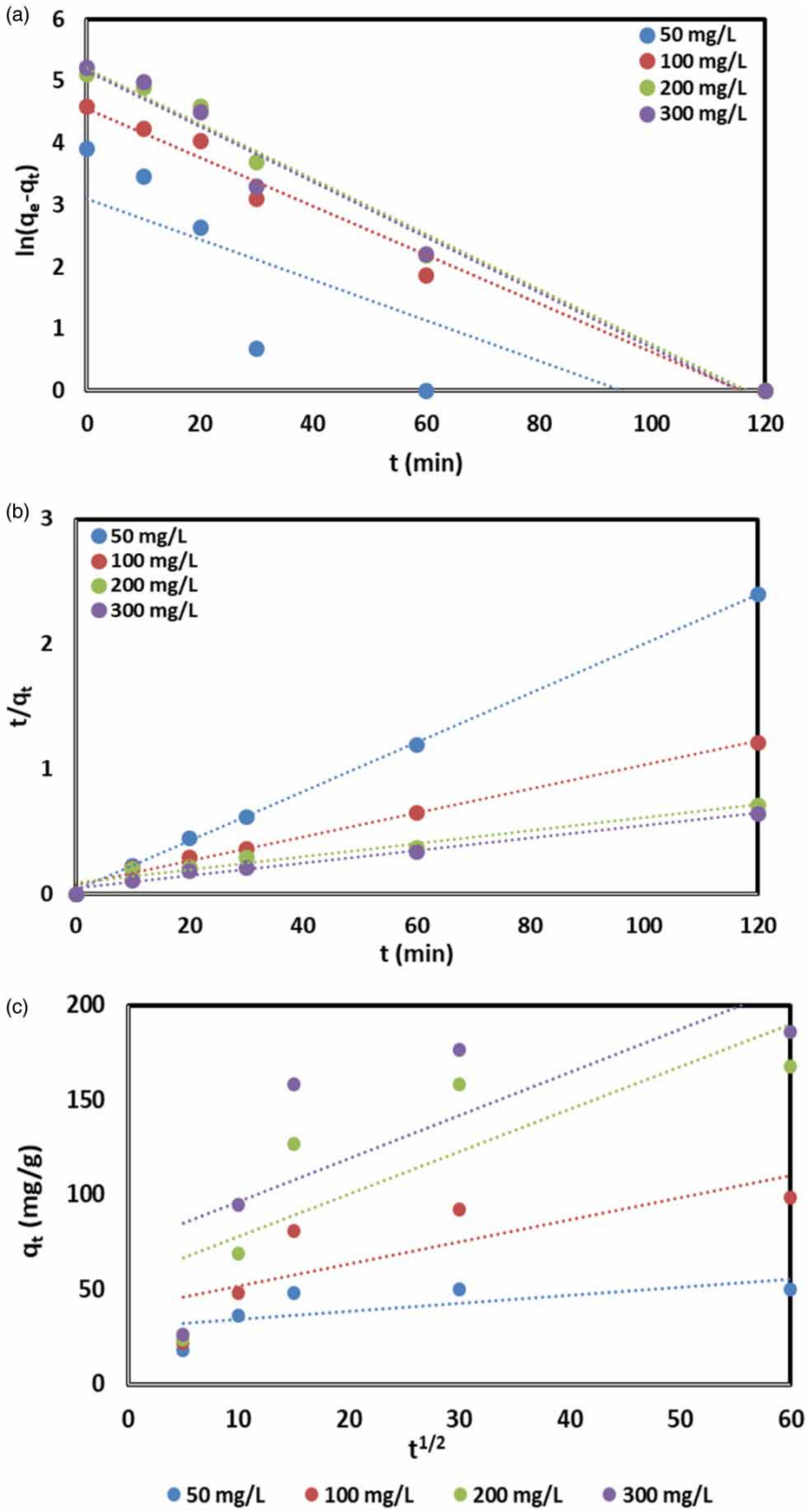

Figure 3 | Linear plot of (a) PFO and (b) PSO, (c) intraparticle diffusion of MB adsorption onto PSCG.

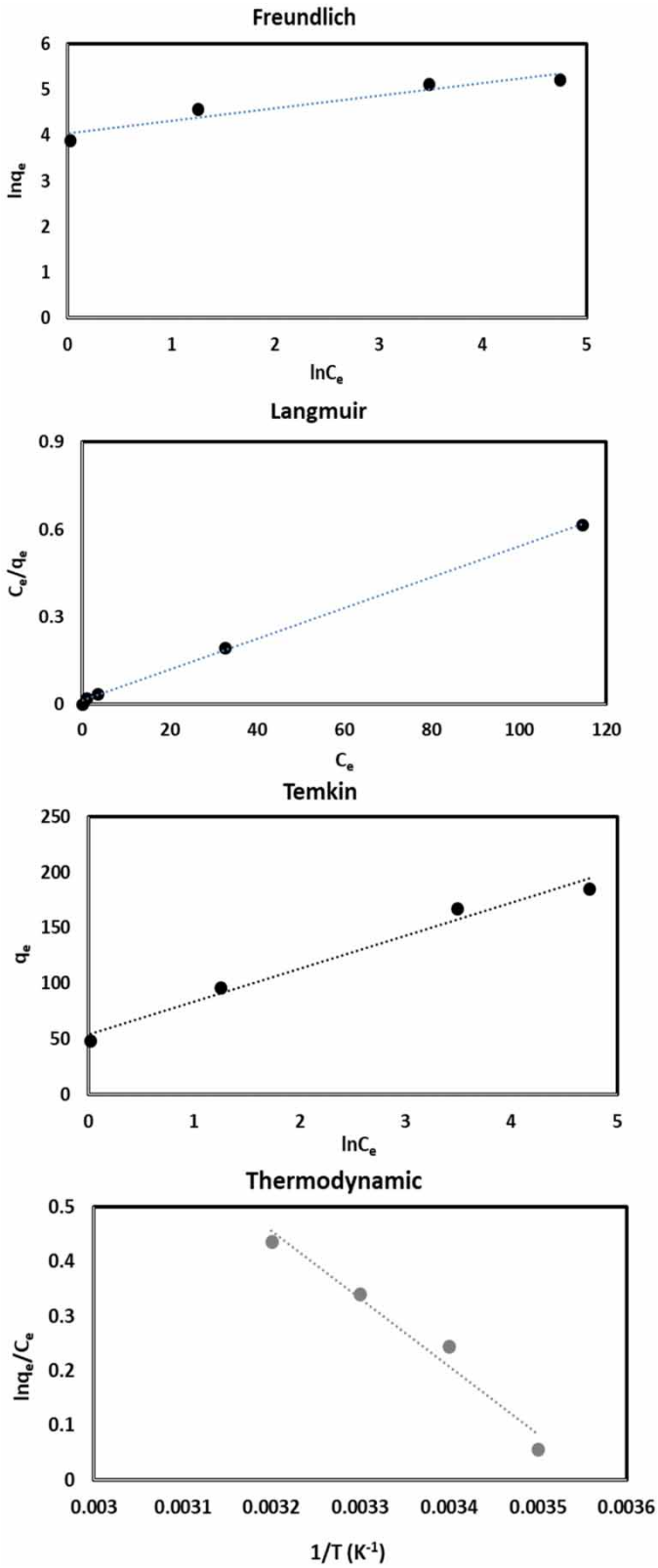

Figure 4 | Linear plot of Freundlich, Langmuir, Temkin and thermodynamics of MB adsorption onto PSCG.

and 0.28, respectively. This confirmed that PSCG had excellent ability to adsorb MB and exhibited excellent performance under various conditions. Moreover, the Temkin constant (B) was calculated as 29.45 (J/mol) and the adsorption of MB by PSCG was closer to chemisorption ($B > 20$ J/mol) than physical adsorption due to the change in the properties of the adsorbent by chemical substances (Table 3).

Temperature affects the adsorption equilibrium and adsorption rate as it affects the solubility of molecules and the diffusion of adsorbent materials within the pores (Choi 2022). The calculated thermodynamic parameters are represented in Table 4 and depicted in Figure 4. The negative ΔG° confirmed that the adsorption of MB onto PSCG was spontaneous and thermodynamically favorable. The positive ΔH° and ΔS° values showed that the adsorption process was endothermic in nature, and designated the affinity of PSCG and MB and increased disorder at the solid/liquid interface during the adsorption process.

The q_m of the Langmuir model is the maximum adsorbent capacity per unit mass of adsorbent, and adsorption capacity is a key parameter for evaluating the adsorption effect of an adsorbent (Leng *et al.* 2019; Yang *et al.* 2020). The maximum adsorption capacity of PSCG was 188.68 mg/g; Table 5 shows the comparison of the maximum adsorption capacity of various adsorbents based on these research results. Although the adsorption capacity of MB using PSCG did not boast a very high adsorption capacity compared to some modified lignocellulose adsorbents, it showed an adequate adsorption capacity with an appropriate amount of adsorbent. Comparison of adsorption capacity with various adsorbents showed that PSCG was a promising adsorbent for the removal of MB.

Adsorption mechanism

Various functional groups on the adsorbent surface play important roles in binding the adsorbent surface to the adsorbate (Gomora-Hernandez *et al.* 2020). There are various functional groups that can adsorb metal cations, as reported in the literature (Leng *et al.* 2019; Qiao *et al.* 2021). For example, O- or N- donors can attract hydrogen bonds and electrostatically attract harmful substances in aqueous solution due to a single pair of oxygen or nitrogen atoms (Zhuang *et al.* 2020; Choi *et al.* 2021; Elgarahy *et al.* 2021). Therefore, polymers containing carboxylic acids and phosphonic acids have been widely used to adsorb various cations such as heavy metals and dyes (Leng *et al.* 2019; Qiao *et al.* 2021). PSCG, a strong acid resin, adsorbs almost all cations contained in the aqueous solution by exchanging hydrogen ions due to the phosphoric acid group contained in the adsorbent. Since this ion exchange process is reversible, resins can be regenerated using strong acids when the ion exchange capacity is exhausted.

In FT-IR analysis, the amount of carboxyl (–COOH) and hydroxyl (-OH) functional groups of PSCG increased, and similar groups such as $P=O$ and $P=OOH$ attached to the PSCG surface interacted with MB ions in aqueous solution. Therefore, the adsorption of MB ions by the modified PSCG was achieved by the surface complexing mechanism between the oxygen-containing functional group and MB ions, which can be summarized as hydrogen bonding, electrostatic attraction, and π-π tracking interaction (Figure 5).

Analysis by FT-IR and SEM showed that phosphorylation increased the porosity and surface area of PSCG. In addition, the phosphoric acid group increased the exposure of anions on the surface by expanding the pore shape of the adsorbent, and as a result, the adsorption efficiency of MB, a cationic ion, for PSCG was improved. Elgarahy *et al.* (2021) reported that phosphoric acid-containing surface groups are important for the adsorption of MBs in solution. These results were consistent with the previously discussed results showing that the adsorption capacity of MB clearly correlates with the amounts of carboxylic groups and phosphate and pyrophosphate groups, respectively. The process of adsorbing MB using an adsorbent modified with phosphoric acid in aqueous solution can be summarized as follows.

Table 4 | Thermodynamic parameters for MB adsorption onto PSCG

Thermodynamic parameters			
T	ΔG°	ΔH°	ΔS°
288	−0.2843	10.301	0.036
298	−0.6519		
308	−1.0194		
318	−1.3870		

Table 5 | The maximum adsorption capacity of MB using various adsorbents

Materials		pH	q_{max} (mg/g)	References
Phosphoric acid treated biomass	*Eucalyptus*	7	977.0	Han *et al.* (2020)
	Agave salmiana leaves	7	200.0	Canales-Flores & Prieto-Carcía (2020)
	Mangosteen peels	6	871.5	Zhang *et al.* (2021)
	Orange peels	7	307.6	Guediri *et al.* (2020)
	Sisal hempulp	7	490.9	Liu *et al.* (2021a)
	Sterculia foetida	7	181.8	Basu *et al.* (2018)
	Banana stem	7	101.0	Misran *et al.* (2022)
	PSCG	7	188.7	This study
Spiky sweetgum tree seeds		7	143.5	Liu *et al.* (2021b)
Natural *Carica papaya* wood		6	32.3	Rangabhahiyam *et al.* (2018)
Microalgae *Scenedesmus*		7	87.0	Afshariani & Roosta (2019)
Palm waste		7	12	Azoulat *et al.* (2020)
Banana peels		7	18.6	Amel *et al.* 2012

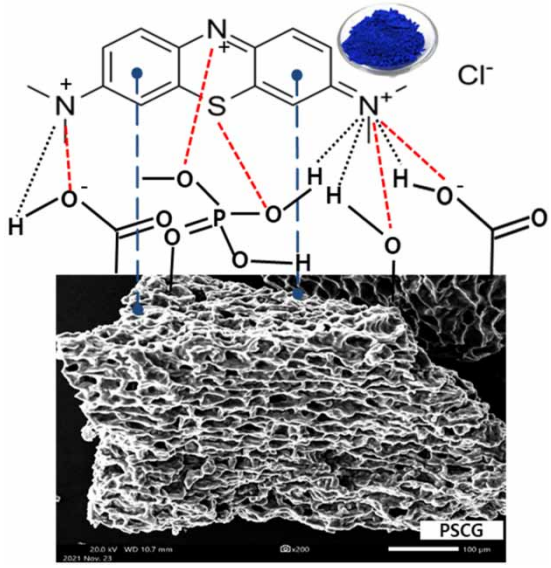

Figure 5 | A possible mechanism of MB adsorption by PSCG; hydrogen bonding (·····), electrostatic attraction (·····) and π–π stacking interaction (·····).

$$PSCG - OH + C_{16}H_{18}ClN_3S{\cdot}3H_2O \rightarrow PSCG - O - C_{16}H_{18}N_3S + HCl + 3H_2O$$
$$PSCG - NH_2 + C_{16}H_{18}ClN_3S{\cdot}3H_2O \rightarrow PSCG - NH - C_{16}H_{18}N_3S + HCl + 3H_2O$$
$$PSCG - COOH + C_{16}H_{18}ClN_3S{\cdot}3H_2O \rightarrow PSCG - COO - C_{16}H_{18}N_3S + HCl + 3H_2O$$
$$PSCG - SO_3H + C_{16}H_{18}ClN_3S{\cdot}3H_2O \rightarrow PSCG - SO_3 - C_{16}H_{18}N_3S + HCl \ + 3H_2O$$
$$PSCG - PO_3H + C_{16}H_{18}ClN_3S{\cdot}3H_2O \rightarrow PSCG - PO_3 - C_{16}H_{18}N_3S + HCl + 3H_2O$$

Reusability of PSCG

As a result of the reuse test, PSCG showed excellent performance with a high removal efficiency of 90% up to four consecutive uses. MB removal efficiency of the reused PSCG decreased to 76.5% after five consecutively times and decreased sharply to 52.4% when used the 6th time (Figure 6). According to previous studies (Leng *et al.* 2019; Han *et al.* 2020; Choi *et al.* 2021), desorption was performed using HCl or NaOH for recovery of used the adsorbent. However, PSCG showed more than 90% removal efficiency up to four times without the desorption process. These results confirm that there was no doubt that PSCG

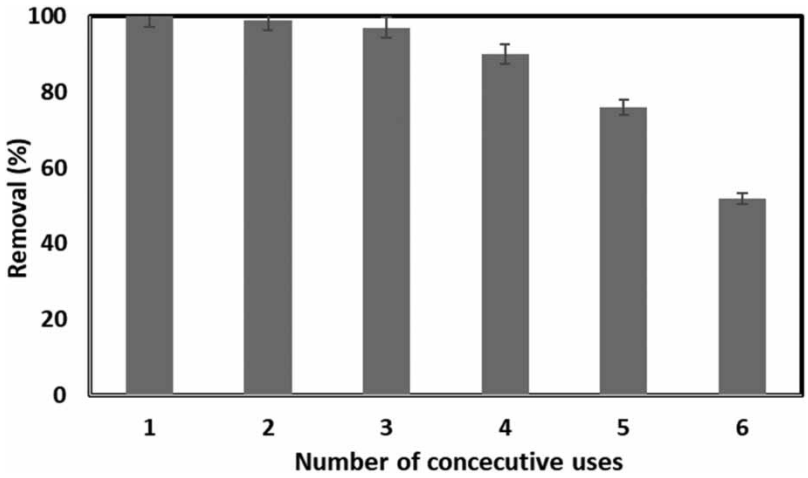

Figure 6 | Reusability of PSCG adsorbent.

was a promising adsorbent for MB adsorption. Adsorbent reusability is an important factor in determining commercial viability for industrial applications. In addition, the availability of coffee grounds, an abundant lignocellulose-based biosorbent that is readily available everywhere, is another key factor in ensuring the continuity of PSCG production. Moreover, the modification method applied to production has the advantage that it is very simple.

CONCLUSIONS

In this study, phosphorylated coffee grounds, a mass-produced waste was used to adsorb MB through various parameters in aqueous solution. The experimental results were analyzed by adsorption isotherms and adsorption kinetics, and the properties of adsorbents were used to explain the adsorption mechanism. After activation with phosphoric acid, PSCG had a mesopore range of 96.9%, confirming that the pore size of the adsorbent and the surface area of the adsorbent were overall increased. According to the results of EDS and pHpzc analysis, it was confirmed that acidic groups were strongly attached to the surface of PSCG. 1 g/L of PSCG adsorbent was able to remove 99% within 20 minutes, and the adsorption efficiency of MB for PSCG was 2.5–3.5 times higher than that of SCG, and it was confirmed that maximum adsorption was reached within a short time. The MB adsorption process in aqueous solution using PSCG was more suitable for the PSO and Langmuir models, and the adsorption process was closer to chemisorption than physical adsorption. The maximum MB adsorption capacity for PSCG according to the Langmuir model was 188.68 mg/g. As a result of the reuse test, PSCG showed excellent performance with a high removal efficiency of 90% up to four consecutive uses. FT-IR analysis showed that phosphorylation improved the number of carboxyl groups, and increased porosity and surface area of the adsorbent. In addition, the phosphoric acid group increased the exposure of anions on the surface by expanding the pore shape of the adsorbent, and as a result, the adsorption efficiency of MB, a cationic ion, for PSCG was improved.

ACKNOWLEDGEMENTS

This study was supported by the Basic Science Research Program through the National Research Foundation (NRF) of Korea, funded by the Ministry of Education, Science and Technology (2021R111A305924311).

DECLARATION OF COMPETING INTEREST

The authors declare that they have no conflicts of interest.

STATEMENT OF INFORMED CONSENT, HUMAN/ANIMAL RIGHTS

No conflicts, informed consent, human or animal rights are applicable.

DECLARATION OF AUTHOR CONTRIBUTIONS

All authors whose names are listed in this manuscript certify that they have participated sufficiently in this work to take public responsibility for the content, including participation in the concept, design, data, collection, analysis, writing, and revision of the manuscript.

DATA AVAILABILITY STATEMENT

All relevant data are included in the paper or its Supplementary Information.

REFERENCES

Afshariani, F. & Roosta, A. 2019 Experimental study and mathematical modeling of bioadsorption of methylene blue from aqueous solution in a packed bed of microalgae *Scenedesmus*. *Journal of Cleaner Production* **225**, 133–142.

Amel, K., Hassena, M. A. & Kerroum, D. 2012 Isotherm and kinetics study of biosorption of cationic dye onto banana peels. *Energy Procedia* **19**, 286–295.

Arora, C., Soni, S., Sahu, S., Mittal, J., Kumar, P. & Bajpai, P. K. 2019 Iron based metal organic framework for efficient removal of methylene blue dye from industrial waste. *Journal of Molecular Liquids* **284**, 343–352.

Azoulat, K., Bencheikh, I., Moufti, A., Dahchour, A., Mabrouki, J. & El Hajjaji, S. 2020 Comparative study between static and dynamic adsorption efficiency of dyes by the mixture of palm waste using the central composite design. *Chemical Data Collections* **27**, 100385.

Basu, S., Ghosh, G. & Saha, S. 2018 Adsorption characteristics of phosphoric acid induced activation of bio-carbon: equilibrium, kinetics, thermodynamics and batch adsorber design. *Process Safety and Environmental Protection* **117**, 125–142.

Canales-Flores, R. A. & Prieto-García, F. 2020 Taguchi optimization for production of activated carbon from phosphoric acid impregnated agricultural waste by microwave heating for the removal of methylene blue. *Diamond and Related Materials* **109**, 108027.

Chen, W. H., Du, J. T., Lee, K. T., Ong, H. C., Park, Y. K. & Huang, C. C. 2021 Pore volume upgrade of biochar from spent coffee grounds by sodium bicarbonate during torrefaction. *Chemosphere* **275**, 129999.

Choi, H. J. 2022 Assessment of sulfonation in cornstalk for adsorption of metal-ions from seawater. *Korean Journal of Chemical Engineering* **39** (1), 121–133.

Choi, H. J. & Yu, S. W. 2018 Application of novel hybrid bioadsorbent, tannin/chitosan/sericite, for the removal of Pb(II) toxic ions from aqueous solution. *Korean Journal of Chemical Engineering* **35** (11), 2198–2206.

Choi, H. J. & Yu, S. W. 2019 Biosorption of methylene blue from aqueous solution by agricultural bioadsorbent corncob. *Environmental Engineering Research* **24** (1), 99–106.

Choi, S. S., Choi, T. R. & Choi, H. J. 2021 Surface modification of phosphoric acid–activated carbon in spent coffee grounds to enhance Cu(II) adsorption from aqueous solutions. *Applied Chemistry for Engineering* **32** (5), 589–598.

Elgarahy, A. M., Elwakeel, K. Z., Mohammad, S. H. & Elshoubaky, G. A. 2021 A critical review of biosorption of dyes, heavy metals and metalloids from wastewater as an efficient and green process. *Cleaner Engineering and Technology* **4**, 100209.

Gomora-Hernandez, J. C., del Carreno-de-Leon, M. C., Flores-Alamo, N., del Hernandez-Berriel, M. C. & Fernandez-Valverde, S. M. 2020 Kinetic and thermodynamic study of corncob hydrolysis in phosphoric acid with a low yield of bacterial inhibitors. *Biomass and Bioenergy* **143**, 105830.

Guediri, A., Bouguettoucha, A., Chebli, D., Chafai, N. & Amrane, A. 2020 Molecular dynamic simulation and DFT computational studies on the adsorption performances of methylene blue in aqueous solutions by orange peel-modified phosphoric acid. *Journal of Molecular Structure* **1202**, 127290.

Han, Q., Wang, J., Goodman, B. A., Xie, J. & Liu, Z. 2020 High adsorption of methylene blue by activated carbon prepared from phosphoric acid treated eucalyptus residue. *Powder Technology* **366**, 239–248.

Karami, K., Beram, S. M., Bayat, P., Siadatnasab, F. & Ramezanpour, A. 2022 A novel nanohybrid based on metal–organic framework MIL101 – Cr/PANI/Ag for the adsorption of cationic methylene blue dye from aqueous solution. *Journal of Molecular Structure* **1247**, 131352.

Khnifira, M., El Hamidi, S., Sadiq, M., Simsek, S., Kaya, S., Barka, N. & Abdennouri, M. 2022 Adsorption mechanisms investigation of methylene blue on the (001) zeolite 4A surface in aqueous medium by computational approach and molecular dynamics. *Applied Surface Science* **572**, 151381.

Kouzbour, S., Gourich, B., Gros, F., Vial, C., Allam, F. & Stirib, Y. 2019 Comparative analysis of industrial processes for cadmium removal from phosphoric acid: a review. *Hydrometallurgy* **188**, 222–247.

Kumar, N. & Kumar, R. 2022 Efficient adsorption of methylene blue on hybrid structural phase of moo_3 nanostructures. *Materials Chemistry and Physics* **275**, 125211.

Lee, S. Y. & Choi, H. J. 2021 Efficient adsorption of methylene blue from aqueous solution by sulfuric acid activated watermelon rind (*Citrullus lanatus*). *Applied Chemistry for Engineering* **32** (3), 348–356.

Leng, X., Zhong, Y., Xu, D., Wang, X. & Yang, L. 2019 Mechanism and kinetics study on removal of iron from phosphoric acid by cation exchange resin. *Chinese Journal of Chemical Engineering* **27**, 1050–1057.

Liu, B., Du, C., Chen, J. J., Zhai, J. Y., Wang, Y. & Li, H. L. 2021a Preparation of well-developed mesoporous activated carbon fibers from plant pulp fibers and its adsorption of methylene blue from solution. *Chemical Physics Letters* **771**, 138535.

Liu, F., Cherith, K., Sai, K. V. & Zhang, W. 2021b Conversion of spiky sweetgum tree (*Liquidambar styraciflua*) seeds as into bio-adsorbent: static and dynamic adsorption assessment. *Journal of Hazardous Materials Advances* **1**, 100001.

Misran, E., Bani, O., Situmeang, E. M. & Purba, A. S. 2022 Banana stem based activated carbon as a low-cost adsorbent for methylene blue removal: isotherm, kinetics, and reusability. *Alexandria Engineering Journal* **61**, 1946–1955.

Patil, M. R. & Shrivastava, V. S. 2016 Adsorptive removal of methylene blue from aqueous solution by polyaniline-nickel ferrite nanocomposite: a kinetic approach. *Desalination and Water Treatment* **57** (13), 5879–5887.

Qiao, A., Cui, M., Huang, R., Ding, G., Qi, W., He, Z., Klemes, J. J. & Su, R. 2021 Advances in nanocellulose-based materials as adsorbents of heavy metals and dyes. *Carbohydrate Polymers* **272**, 118471.

Rangabhahiyam, S., Lata, S. & Balasubramanian, P. 2018 Biosorption characteristics of methylene blue and malachite green from simulated wastewater onto Carica papaya wood bioadsorbent. *Surface and Interfaces* **10**, 197–215.

Shi, C., Chen, Y., Yu, Z., Li, S., Chan, H., Suna, S., Chen, G., He, M. & Tian, J. 2021 Sustainable and super hydrophobic spent coffee ground-derived holocellulose nanofibers foam for continuous oil/water separation. *Sustainable Materials and Technologies* **28**, e00277.

Soni, S., Bajpai, P. K., Bharti, D., Mittal, J. & Arora, C. 2020a Removal of crystal violet from aqueous solution using iron based metal organic framework. *Desalination and Water Treatment* **205**, 386–399.

Soni, S., Bajpai, P. K., Mittal, J. & Arora, C. 2020b Utilisation of cobalt doped iron based MOF for enhanced removal and recovery of methylene blue dye from waste water. *Journal of Molecular Liquids* **314**, 113642.

Sych, N. V., Trofymenko, S. I., Poddubnaya, O. I., Tsyba, M. M., Sapsay, V. I., Klymchuk, D. O. & Puziy, A. M. 2012 Porous structure and surface chemistry of phosphoric acid activated carbon from corncob. *Applied Surface Science* **261**, 75–82.

Xu, J., Chen, L., Qu, H., Jiao, Y., Xie, J. & Xing, G. 2014 Preparation and characterization of activated carbon from reedy grass leaves by chemical activation with H_3PO_4. *Applied Surface Science* **320**, 674–680.

Yang, Q., Wu, P., Liu, J., Rehman, S., Ahmed, Z., Ruan, B. & Zhu, N. 2020 Batch interaction of emerging tetracycline contaminant with novel phosphoric acid activated corn straw porous carbon: adsorption rate and nature of mechanism. *Environmental Research* **181**, 108899.

Zeng, H., Zeng, H., Zhang, H., Shahab, A., Zhang, K., Lu, Y., Nabi, I., Naseem, F. & Ullah, H. 2021 Efficient adsorption of Cr (VI) from aqueous environments by phosphoric acid activated eucalyptus biochar. *Journal of Cleaner Production* **286**, 124964.

Zhang, Z., Xu, L., Liu, Y., Feng, R., Zou, T., Zhang, Y., Kang, Y. & Zhou, P. 2021 Efficient removal of methylene blue using the mesoporous activated carbon obtained from mangosteen peel wastes: kinetic, equilibrium, and thermodynamic studies. *Microporous and Mesoporous Materials* **315**, 110904.

Zhuang, H., Zhong, Y. & Yang, L. 2020 Adsorption equilibrium and kinetics studies of divalent manganese from phosphoric acid solution by using cationic exchange resin. *Chinese Journal of Chemical Engineering* **28**, 2758–2770.

Zieliński, J., Huculak-Mączka, M., Kaniewski, M., Nieweś, D., Hoffmann, K. & Hoffmann, J. 2019 Kinetic modelling of cadmium removal from wet phosphoric acid by precipitation method. *Hydrometallurgy* **190**, 10517.

First received 1 December 2021; accepted in revised form 8 January 2022. Available online 24 January 2022